# Exact Hydrodynamics of a Trapped Dipolar Bose-Einstein Condensate

Duncan H. J. O'Dell,[1] Stefano Giovanazzi,[2] and Claudia Eberlein[1]

[1]*Department of Physics and Astronomy, University of Sussex, Falmer, Brighton BN1 9QH, England*
[2]*School of Physics and Astronomy, University of St. Andrews, North Haugh, St. Andrews KY16 9SS, Scotland*

(Received 5 August 2003; published 21 June 2004)

We present exact results in the Thomas-Fermi regime for the statics and dynamics of a harmonically trapped Bose-Einstein condensate that has dipole-dipole interactions in addition to the usual *s*-wave contact interactions. Remarkably, despite the nonlocal and anisotropic nature of the dipolar interactions, the density profile in a general time-dependent harmonic trap is an inverted parabola. The evolution of the condensate radii is governed by local, ordinary differential equations, and as an example we calculate the monopole and quadrupole shape oscillation frequencies.

DOI: 10.1103/PhysRevLett.92.250401 PACS numbers: 03.75.Kk, 32.80.Qk, 34.20.Cf, 75.80.+q

A Bose-Einstein condensate (BEC) whose particles interact via dipole-dipole forces constitutes an example of a superfluid with long-range and anisotropic interparticle interactions. This is in contrast to usual BECs which have isotropic interactions whose range is far less than the average interparticle separation (see [1] for a review). The long-range and anisotropic nature of dipole-dipole interactions has been predicted to lead to BECs with unusual stability properties [2], exotic states such as supersolid and checkerboard phases [3,4], and modified excitation spectra [5], even to the extent of a roton minimum [6]. Alkali atoms typically have small dipole-dipole interactions, but a good candidate for a dipolar BEC is chromium since it has a large magnetic moment of six Bohr magnetons, and there has recently been progress in cooling it towards degeneracy [7]. Molecules can, of course, have huge dipole moments: advances in the cooling of polar molecules [8], photoassociation of ultracold heteronuclear molecules [9], and molecular BECs [10] suggest we might soon see superfluids where dipolar effects dominate.

Here we consider a harmonically trapped BEC that has dipole-dipole interactions as well as short-range *s*-wave scattering. In the Thomas-Fermi limit (where the zero-point kinetic energy of the atoms in the trap is negligible in comparison to the interparticle interaction energy and the trapping potential) the collective dynamics of a BEC are described by the collisionless hydrodynamic theory of Bose superfluids at zero temperature [11]. The dipolar interactions render the already nonlinear hydrodynamic equations nonlocal. Nevertheless, we shall obtain the density profile in the presence of time-dependent harmonic trapping, which is equivalent to the results obtained for ordinary nondipolar BECs by Kagan *et al.* [12] and by Castin and Dum [13]. The solutions for the dynamics provide a general tool, which can be used for analyzing a dipolar BEC, e.g., large amplitude oscillations, or ballistic expansion upon release of the trap (often necessary for imaging the BEC).

The dominant interactions in the ultracold gases created thus far are asymptotically of the van der Waals type, which decay as $r^{-6}$ and are short range in comparison to the average interatomic distance. Within the mean-field regime of the Gross-Pitaevskii equation [1] these interactions are modeled by a pseudopotential, $g\delta(\mathbf{r}) \equiv (4\pi a_s \hbar^2/m)\delta(\mathbf{r})$, where $m$ is the atomic mass, and $g$ incorporates the quantum aspects of low-energy scattering via the *s*-wave scattering length, $a_s$. By using a Feshbach resonance, the value of $a_s$ can be adjusted between positive (repulsive) and negative (attractive) values [14]. Dipolar interactions occur if the atoms are polarized by an electric field [15], or if the atoms possess a magnetic moment [16]. By analogy to nuclear magnetic resonance techniques, dipole-dipole interactions can also be controlled in both magnitude and sign by rapidly rotating an external field [17]—they vanish when the rotation is at the so-called magic angle.

The long-range part of the interaction between two dipoles separated by $\mathbf{r}$, and aligned by an external field along a unit vector $\hat{\mathbf{e}}$, is given by

$$U_{\mathrm{dd}}(\mathbf{r}) = \frac{C_{\mathrm{dd}}}{4\pi}\hat{\mathbf{e}}_i\hat{\mathbf{e}}_j\frac{(\delta_{ij} - 3\hat{\mathbf{r}}_i\hat{\mathbf{r}}_j)}{r^3}. \tag{1}$$

Dipoles induced by an electric field $\mathbf{E} = E\hat{\mathbf{e}}$ have a coupling $C_{\mathrm{dd}} = E^2\alpha^2/\epsilon_0$, where $\alpha$ is the static polarizability, and $\epsilon_0$ the permittivity of free space. For atoms with a magnetic dipole moment $d_m$ aligned by a magnetic field $\mathbf{B} = B\hat{\mathbf{e}}$, one has $C_{\mathrm{dd}} = \mu_0 d_m^2$, where $\mu_0$ is the permeability of free space. A measure of the strength of the dipolar interactions relative to the *s*-wave scattering is given by the dimensionless quantity

$$\varepsilon_{\mathrm{dd}} \equiv \frac{C_{\mathrm{dd}}}{3g}. \tag{2}$$

Note that the value of $g$ can be altered by the presence of a strong electric field [5]. The definition (2) arises naturally from an analysis of the frequencies of collective excitations in a homogeneous dipolar BEC: for $\varepsilon_{\mathrm{dd}} > 1$ instabilities can occur in the hydrodynamic limit [16,17].

  

Alkali atoms can have a magnetic dipole moment of $d_m = 1\mu_B$ (Bohr magneton), and for $^{87}$Rb, which has $a_s \approx 103a_0$ (Bohr radius), $\varepsilon_{dd} \approx 0.007$. Na has $\varepsilon_{dd} \approx 0.004$, and accordingly magnetic dipolar effects in BECs of these atoms are small, at least in a stationary condition: the effects of dipolar interactions can be made visible by rotating the magnetic field in resonance with a collective excitation frequency of the system [17]. Also, using a Feshbach resonance to reduce $a_s$ could substantially increase $\varepsilon_{dd}$ [18]. Chromium, on the other hand, has $d_m = 6\mu_B$. The more common bosonic isotope, $^{52}$Cr, has $a_s = 170 \pm 40a_0$ [7], giving $\varepsilon_{dd} \approx 0.089$. The less common bosonic isotope $^{50}$Cr has $a_s = 40 \pm 15a_0$ [7], and $\varepsilon_{dd} \approx 0.36$ is much higher. Using a crossed optical trap, atom numbers in a $^{52}$Cr BEC on the order of $N = 10^4$ might be within reach, and the frequencies of the harmonic confinement would be in the region of $\omega_x = \omega_y = 2\pi 170\ \mathrm{s}^{-1}$ and $\omega_z = 2\pi 240\ \mathrm{s}^{-1}$ [19]. The trap anisotropy $\gamma = \omega_z/\omega_x = 1.41$ is optimal for enhancing the condensate shape deformations [20]. For a trapped BEC with just $s$-wave scattering the Thomas-Fermi limit is reached for large values of the parameter $Na_s/a_{ho}$ [1], where $a_{ho} = \sqrt{\hbar/m\omega}$ is the harmonic oscillator length of the trap, and $N$ is the total number of atoms. For $^{52}$Cr one has $Na_s/a_{ho} \approx 10^2$, illustrating that an analysis within the Thomas-Fermi regime is appropriate for these experiments.

Collisionless hydrodynamics derives from the existence of a macroscopic condensate order parameter $\psi(\mathbf{r}, t) = \sqrt{n(\mathbf{r}, t)}\exp i\phi(\mathbf{r}, t)$, normalized to $N$, consisting of density $n(\mathbf{r}, t)$, and phase $\phi(\mathbf{r}, t)$. The phase determines the superfluid velocity via potential flow, $\mathbf{v}(\mathbf{r}, t) = (\hbar/m)\nabla\phi(\mathbf{r}, t)$. The nonlinear evolution of a nondipolar BEC in the Thomas-Fermi regime is dictated by the continuity and Euler equations given by, respectively,

$$\frac{\partial n}{\partial t} = -\nabla\cdot(n\mathbf{v}), \tag{3}$$

$$m\frac{\partial \mathbf{v}}{\partial t} = -\nabla\left(\frac{mv^2}{2} + V_{ext} + gn\right). \tag{4}$$

$V_{ext}$ is the external potential, which is provided by the harmonic trap, $V_{ext}(\mathbf{r}) = m(\omega_x^2x^2 + \omega_y^2y^2 + \omega_z^2z^2)/2$. Equations (3) and (4) are equivalent to the time-dependent Gross-Pitaevskii equation [1] when a zero-point fluctuation term $(-\hbar^2\nabla^2\sqrt{n}/2m\sqrt{n})$ is included in the brackets on the right-hand side (rhs) of (4). The equilibrium solution of (3) and (4), which has $\mathbf{v} = 0$, is the well-known Thomas-Fermi inverted parabola, $n(\mathbf{r}) = [\mu - V_{ext}(\mathbf{r})]/g$ for $n(\mathbf{r}) \geq 0$, and $n(\mathbf{r}) = 0$ elsewhere. $\mu$ is the chemical potential. The density profile is completely determined by the trapping potential and has the same aspect ratio as the trap.

Motivated by the experimental possibility of changing the trapping frequencies in time, so that $\omega_j \to \omega_j(t)$ with $j = x, y, z$, Refs. [12,13] studied a special class of an exact "scaling" solution to (3) and (4) for time-dependent harmonic traps, corresponding to [1]

$$n(\mathbf{r}, t) = n_0(t)\left[1 - \frac{x^2}{R_x^2(t)} - \frac{y^2}{R_y^2(t)} - \frac{z^2}{R_z^2(t)}\right], \tag{5}$$

$$\mathbf{v}(\mathbf{r}, t) = \frac{1}{2}\nabla[\alpha_x(t)x^2 + \alpha_y(t)y^2 + \alpha_z(t)z^2], \tag{6}$$

for $n(\mathbf{r}, t) \geq 0$, and $n(\mathbf{r}, t) = 0$ elsewhere. $n_0(t) = 15N/[8\pi R_x(t)R_y(t)R_z(t)]$ is the central density. The time evolution of the radii $R_j$ is governed by three *ordinary* differential equations, and $\alpha_j = \dot{R}_j/R_j$.

*Exact static solution for a Thomas-Fermi dipolar BEC.*—The simplicity of the inverted-parabola solution (5) and (6) relies upon the local character of $s$-wave contact interactions to give a mean-field potential $gn(\mathbf{r})$. Dipolar interactions, on the other hand, are long range and give rise to a potential [5]

$$\Phi_{dd}(\mathbf{r}) \equiv \int d^3r' U_{dd}(\mathbf{r} - \mathbf{r}')n(\mathbf{r}'). \tag{7}$$

The hydrodynamic equations for a dipolar BEC are the same as given in (3) and (4), but with (4) supplemented by adding $\Phi_{dd}(\mathbf{r})$ into the bracket on the rhs. Using the identity $[(\delta_{ij} - 3\hat{r}_i\hat{r}_j)/4\pi r^3] = -\nabla_i\nabla_j(1/4\pi r) - \frac{1}{3}\delta_{ij}\delta(\mathbf{r})$, we can rewrite (7) as

$$\Phi_{dd}(\mathbf{r}) = -C_{dd}\left(\hat{\mathbf{e}}_i\hat{\mathbf{e}}_j\nabla_i\nabla_j\phi(\mathbf{r}) + \frac{1}{3}n(\mathbf{r})\right), \tag{8}$$

with

$$\phi(\mathbf{r}) \equiv \frac{1}{4\pi}\int\frac{d^3r' n(\mathbf{r}')}{|\mathbf{r} - \mathbf{r}'|}. \tag{9}$$

We thereby reduce the dipolar problem to an analogy with electrostatics, involving the "potential" $\phi(\mathbf{r})$ arising from the "static charge" distribution $n(\mathbf{r})$. Indeed, $\phi(\mathbf{r})$ given by (9) obeys Poisson's equation, $\nabla^2\phi = -n(\mathbf{r})$. The integral (9) can therefore be calculated by using methods such as the Green's functions for Poisson's equation in a coordinate system appropriate to the boundary conditions set by the form of $n(\mathbf{r})$. The surprising result that this form should also be parabolic can be seen from the following argument: if the density is parabolic then Poisson's equation is satisfied by a potential $\phi = a_0 + a_1x^2 + a_2y^2 + a_3z^2 + a_4x^2y^2 + a_5x^2z^2 + a_6y^2z^2 + a_7x^4 + a_8y^4 + a_9z^4$. By inserting this $\phi$ into (8) one sees that the dipolar mean-field potential, $\Phi_{dd}(\mathbf{r})$, is also parabolic. Therefore, in a harmonic trap, all the terms in the bracket on the rhs of the Euler equation are either quadratic or constants, just as in the simple $s$-wave only case, and remarkably an inverted parabola remains a self-consistent solution to the *dipolar* hydrodynamic equations.

For simplicity (though not necessity), we restrict attention to cylindrical symmetry for both trap and BEC about the $z$ axis, along which the applied polarizing field is taken to point. Thus $R_x = R_y$ and $V_{ext} = (m/2)[\omega_x^2\rho^2 + \omega_z^2z^2]$, where $\rho^2 = x^2 + y^2$. The evaluation of the integral

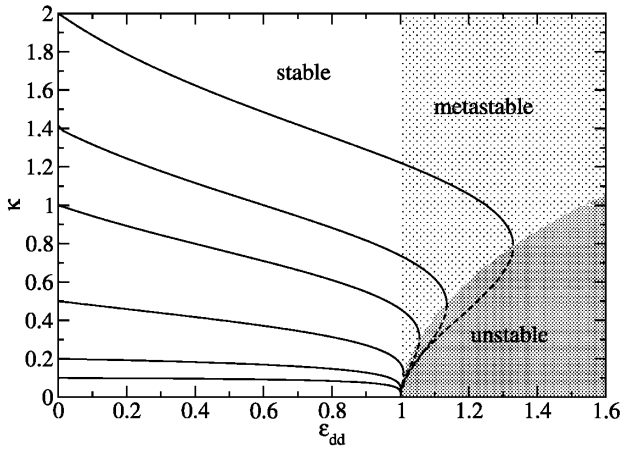


FIG. 1. Aspect ratio $\kappa$ of the parabolic solution as a function of $\varepsilon_{dd}$. Each line is for a different trap aspect ratio $\gamma$ ($\kappa = \gamma$ when $\varepsilon_{dd} = 0$). When $0 < \gamma[\kappa] < 1$ the trap [condensate] is prolate, $\gamma[\kappa] > 1$ the trap [condensate] is oblate. Dashed lines indicate unstable branches. Note, however, that short-wavelength phonons can also cause instabilities if $\varepsilon_{dd} > 1$.

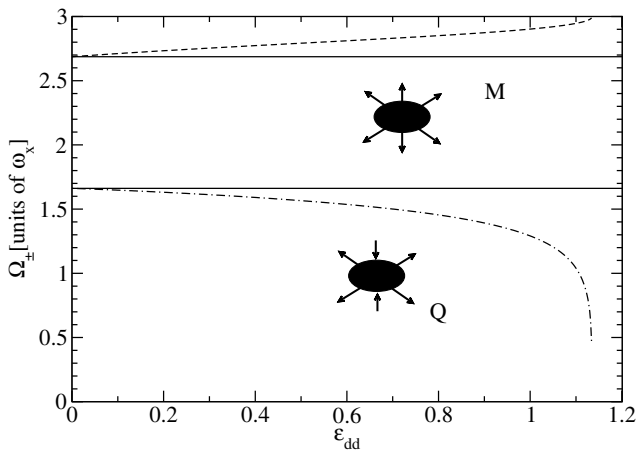


FIG. 2. The monopole (dashed line) and quadrupole (dash-dotted line) oscillation frequencies as functions of $\varepsilon_{dd}$. The trap aspect ratio is set at $\gamma = 240/170$. The solid lines are for $s$-wave contact interactions only, $\Omega^0_{\pm}$. The frequencies become complex at the value of $\varepsilon_{dd}$ at which the equilibrium solution (12) becomes unstable to scaling perturbations, but other instabilities, such as phonons, can also arise when $\varepsilon_{dd} > 1$.

(9) over the inverted-parabola (5) density distribution can be achieved using Green's functions in spheroidal coordinates. We give this calculation elsewhere [21]. The result is a potential (8) inside the condensate region, given by

$$\Phi_{dd} = \frac{n_0 C_{dd}}{3}\left[\frac{\rho^2}{R_x^2} - \frac{2z^2}{R_z^2} - f(\kappa)\left(1 - \frac{3}{2}\frac{\rho^2 - 2z^2}{R_x^2 - R_z^2}\right)\right], \tag{10}$$

where

$$f(\kappa) = \frac{1 + 2\kappa^2}{1 - \kappa^2} - \frac{3\kappa^2 \operatorname{arctanh}\sqrt{1 - \kappa^2}}{(1 - \kappa^2)^{3/2}}, \tag{11}$$

and $\kappa \equiv R_x/R_z$ is the condensate aspect ratio. We recover the result (9) of [17] in the particular case of spherical symmetry ($R_x = R_z$). We have also checked (10) and (11) by direct numerical integration of (7).

To determine the equilibrium values of the radii, the result (10) for $\Phi_{dd}$ should be substituted into the Euler Eq. (4) with $\mathbf{v} = 0$, giving

$$R_x = R_y = \left[\frac{15gN\kappa}{4\pi m\omega_x^2}\left\{1 + \varepsilon_{dd}\left(\frac{3}{2}\frac{\kappa^2 f(\kappa)}{1 - \kappa^2} - 1\right)\right\}\right]^{1/5} \tag{12}$$

and $R_z = R_x/\kappa$. The value of the aspect ratio $\kappa$ is given by the solution of a transcendental equation [5,20]

$$\frac{\kappa^2}{\gamma^2}\left[\frac{3\varepsilon_{dd} f(\kappa)}{1 - \kappa^2}\left(\frac{\gamma^2}{2} + 1\right) - 2\varepsilon_{dd} - 1\right] = \varepsilon_{dd} - 1, \tag{13}$$

where $\gamma = \omega_z/\omega_x$ is the ratio of the trapping frequencies. Figure 1 shows the dependence of $\kappa$ upon $\varepsilon_{dd}$ for various trap aspect ratios. Dipole-dipole forces polarized along $z$ cause an elongation of the BEC along this axis. For an oblate trap ($\gamma > 1$) the BEC becomes spherical when $\varepsilon_{dd} = (5/2)(\gamma^2 - 1)/(\gamma^2 + 2)$.

An analysis of the energy functional associated with the scaling solution (5) shows that when $\varepsilon_{dd} > 1$ the solution loses its global stability to *scaling* perturbations and is only metastable [2,5] (only a local minimum of the energy, the global minimum being a collapsed pencil-like prolate state). Increasing $\varepsilon_{dd}$ further, the scaling solution ceases to exist entirely in the region marked as unstable in Fig. 1. However, we caution the reader that as one enters the region where $\varepsilon_{dd} > 1$ an inverted-parabola scaling solution also becomes unstable to phonons with wavelengths much smaller than the size of the BEC [21], similarly to the homogenous case. Our solutions are therefore unlikely to remain accurate outside the stable region, and the figures extend beyond $\varepsilon_{dd} = 1$ only to indicate the influence of the instability in organizing the

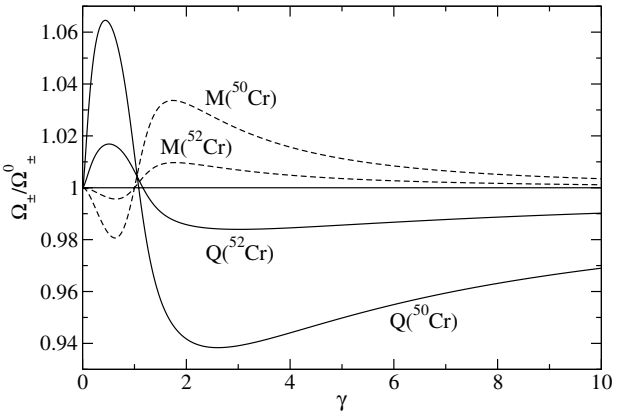


FIG. 3. The monopolar (dashed line) and quadrupolar (solid line) frequencies as fractions of their $s$-wave-only frequencies, $\Omega^0_{\pm}$, for $^{52}$Cr ($\varepsilon_{dd} = 0.089$) and $^{50}$Cr ($\varepsilon_{dd} = 0.36$), plotted as functions of the trap anisotropy $\gamma$.

solutions in the stable region. In order to obtain an accurate picture for $\varepsilon_{\rm dd} \geq 1$ it is necessary to include the zero-point fluctuation term neglected in Eq. (4).

*Exact hydrodynamics of a dipolar condensate.*—Substituting (5) and (6) into the continuity and Euler equations yields the equations of motion for the radii

$$\ddot{R}_x = -\omega_x^2(t)R_x + \frac{15gN}{4\pi m R_x R_z}\left[\frac{1}{R_x^2} - \varepsilon_{\rm dd}(t)\left(\frac{1}{R_x^2} + \frac{3}{2}\frac{f(R_x/R_z)}{R_x^2 - R_z^2}\right)\right], \tag{14}$$

$$\ddot{R}_z = -\omega_z^2(t)R_z + \frac{15gN}{4\pi m R_x^2}\left[\frac{1}{R_z^2} + 2\varepsilon_{\rm dd}(t)\left(\frac{1}{R_z^2} + \frac{3}{2}\frac{f(R_x/R_z)}{R_x^2 - R_z^2}\right)\right]. \tag{15}$$

These equations for the dynamics are exact, and together with the equilibrium radii (12), form the main results of this paper. They provide an efficient way to calculate the evolution of a dipolar BEC in a time-dependent trap [$\omega_j(t)$], including ballistic expansion if the trap is turned off [18,20]. Another possibility is time-dependent dipolar coupling [$\varepsilon_{\rm dd}(t)$], which can be realized by modulating the polarizing field in time. This can be used, e.g., to parametrically excite the quadrupole shape oscillation mode [17]. Such an experiment would allow a determination of $\varepsilon_{\rm dd}$. If the trap is turned off, the $s$-wave and dipolar interaction energies are converted into kinetic energy, the so-called release energy, which can be measured in an experiment. We find $E_{\rm rel} = 15gN^2[1 - \varepsilon_{\rm dd} f(\kappa)]/(28\pi R_x^2 R_z)$, where $\kappa$, $R_x$, and $R_z$ are the equilibrium values calculated from (13) and (12).

Linearizing (14) and (15) around the static solution (12) gives the frequencies for small amplitude oscillations

$$\Omega_\pm^2 = \frac{\omega_x^2}{2}[h_{xx} + h_{zz} \pm \sqrt{(h_{xx} - h_{zz})^2 + 4h_{xz}h_{zx}}], \qquad h_{xx} = 1 + 3\left(1 - \varepsilon_{\rm dd}\left[\frac{1 - 2\kappa^2}{1 - \kappa^2} + \frac{\kappa^2(4\kappa^2 + 1)f(\kappa)}{2(1 - \kappa^2)^2}\right]\right)\Big/\Lambda,$$
$$h_{zz} = \gamma^2 + 2\kappa^2\left(1 + \varepsilon_{\rm dd}\left[\frac{5 - 2\kappa^2}{1 - \kappa^2} - \frac{3(\kappa^2 + 4)f(\kappa)}{2(1 - \kappa^2)^2}\right]\right)\Big/\Lambda, \qquad h_{zx} = 2h_{xz} = 2\kappa\left(1 - \varepsilon_{\rm dd}\left[\frac{1 + 2\kappa^2}{1 - \kappa^2} - \frac{15\kappa^2 f(\kappa)}{2(1 - \kappa^2)^2}\right]\right)\Big/\Lambda, \tag{16}$$

where $\Lambda = 1 + \varepsilon_{\rm dd}[3\kappa^2 f(\kappa)/(2 - 2\kappa^2) - 1]$. $\Omega_-$ corresponds to quadrupole, and $\Omega_+$ to monopole (breathing) shape oscillations, respectively [5]; see Fig. 2. Certain trap anisotropies maximize the effects of dipolar interactions upon the frequencies, as shown in Fig. 3.

*Conclusion.*—The versatility of quantum gases makes them good systems to study the role of interactions in superfluidity. We have solved the dipolar superfluid hydrodynamic equations in a harmonic trap: the condensate density is parabolic, like in the pure $s$-wave case but with modified radii. The evolution of the radii due to a time-dependent harmonic trap/dipolar interaction is given by Eqs. (14) and (15), which therefore represent a valuable tool for the analysis of upcoming experiments.

We thank Tilman Pfau and his group for sharing their results with us. We acknowledge financial support from the EPSRC (UK), the EC, and the Royal Society.

[1] F. Dalfovo, S. Giorgini, L. P. Pitaevskii, and S. Stringari, Rev. Mod. Phys. **71**, 463 (1999).
[2] L. Santos, G.V. Shlyapnikov, P. Zoller, and M. Lewenstein, Phys. Rev. Lett. **85**, 1791 (2000); P. M. Lushnikov, Phys. Rev. A **66**, 051601(R) (2002).
[3] S. Giovanazzi, D. O'Dell, and G. Kurizki, Phys. Rev. Lett. **88**, 130402 (2002).
[4] K. Góral, L. Santos, and M. Lewenstein, Phys. Rev. Lett. **88**, 170406 (2002).
[5] S. Yi and L. You, Phys. Rev. A **63**, 053607 (2001); **66**, 013607 (2002); K. Góral and L. Santos, *ibid.* **66**, 023613 (2002).
[6] D. H. J. O'Dell, S. Giovanazzi, and G. Kurizki, Phys. Rev. Lett. **90**, 110402 (2003); L. Santos, G.V. Shlyapnikov, and M. Lewenstein, *ibid.* **90**, 250403 (2003).
[7] P. O. Schmidt *et al.*, Phys. Rev. Lett. **91**, 193201 (2003); S. Hensler *et al.*, Appl. Phys. B **77**, 765 (2003); J. D. Weinstein, R. deCarvalho, C. I. Hancox, and J. M. Doyle, Phys. Rev. A **65**, 021604 (2002).
[8] J. D. Weinstein *et al.*, Nature (London) **395**, 148 (1998); H. L. Bethlem, G. Berden, and G. Meijer, Phys. Rev. Lett. **83**, 1558 (1999); H. L. Bethlem *et al.*, Nature (London) **406**, 491 (2000); H. L. Bethlem *et al.*, Phys. Rev. A **65**, 053416 (2002).
[9] M.W. Mancini *et al.*, Phys. Rev. Lett. **92**, 133203 (2004).
[10] M. Greiner, C. A. Regal, and D. S. Jin, Nature (London) **426**, 537 (2003); S. Jochim *et al.*, Science **302**, 2101 (2003); M.W. Zwierlein *et al.* Phys. Rev. Lett. **91**, 250401 (2003).
[11] S. Stringari, Phys. Rev. Lett. **77**, 2360 (1996).
[12] Yu. Kagan, E. L. Surkov, and G.V. Shlyapnikov, Phys. Rev. A **54**, R1753 (1996); **55**, R18 (1997).
[13] Y. Castin and R. Dum, Phys. Rev. Lett. **77**, 5315 (1996).
[14] S. Inouye *et al.*, Nature (London) **392**, 151 (1998).
[15] S. Yi and L. You, Phys. Rev. A **61**, 041604 (2000).
[16] K. Góral, K. Rzążewski, and T. Pfau, Phys. Rev. A **61**, 051601 (2000); J.-P. Martikainen, M. Mackie, and K.-A. Suominen, Phys. Rev. A **64**, 037601 (2001).
[17] S. Giovanazzi, A. Görlitz, and T. Pfau, Phys. Rev. Lett. **89**, 130401 (2002).
[18] S. Yi and L. You, Phys. Rev. A **67**, 045601 (2003).
[19] S. Hensler and T. Pfau (private communication).
[20] S. Giovanazzi, A. Görlitz, and T. Pfau, J. Opt. B **5**, S208 (2003).
[21] C. Eberlein, S. Giovanazzi, and D. H. J. O'Dell, cond-mat/0311100.